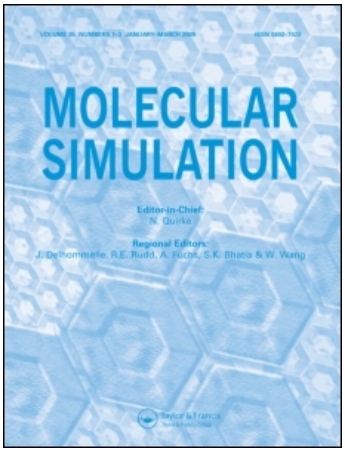

Molecular Simulation
Publication details, including instructions for authors and subscription information:
http://www.informaworld.com/smpp/title~content=t713644482

Solvation Force and Confinement-Induced Phase Transitions of Model Ultra Thin Films

Philippe Bordarier[a]; Bernard Rousseau[a]; Alain H. Fuchs[a]
[a] Laboratoire de Chimie-Physique des Matériaux Amorphes, (URA 1104 CNRS), Btiment 490, Université Paris-Sud, Orsay, France

To cite this Article Bordarier, Philippe , Rousseau, Bernard and Fuchs, Alain H.(1996) 'Solvation Force and Confinement-Induced Phase Transitions of Model Ultra Thin Films', Molecular Simulation, 17: 4, 199 — 215
To link to this Article: DOI: 10.1080/08927029608024109
URL: http://dx.doi.org/10.1080/08927029608024109

Molecular Simulation, 1996, Vol. 17, pp. 199–215
Reprints available directly from the publisher
Photocopying permitted by license only

SOLVATION FORCE AND CONFINEMENT-INDUCED PHASE TRANSITIONS OF MODEL ULTRA THIN FILMS

PHILIPPE BORDARIER, BERNARD ROUSSEAU
and ALAIN H. FUCHS*

Laboratoire de Chimie-Physique des Matériaux Amorphes, (URA 1104 CNRS), Bâtiment 490, Université Paris-Sud, 91405 Orsay, France

(Received December 1995; accepted April 1996)

The static (equilibrium) properties of atomically thin films confined between two surfaces are studied as a function of surface separation by Grand Canonical Monte Carlo and Molecular Dynamics simulations. A model was used, in which the fluid and wall species consist of two different Lennard-Jones rare gas atoms. This was designed to mimic the static SFA experiments in which it is known that epitaxy is not necessary for inducing an oscillatory solvation force in simple non polar liquids. We have been able to simulate, using this simple system, many aspects of the equilibrium properties observed in the experiments. The solvation force is an exponentially damped, periodic curve. All peaks of maximum amplitude in the solvation force correspond to solid-like structures. These structures melt in increasing the surface separation. A further increase in separation leads to the addition of a whole layer and the recrystallisation of the film. In addition this model displays an interesting phenomenon of confinement induced solid-solid phase transition. Two different stable packing (bcc and triclinic) can be observed in the bilayer film and a transition from one to the other occurs when the surface separation is changed. This phase change has been studied as a function of pressure and temperature. As compared to the simulations using a 'commensurate' model, in which the fluid and wall species are made of like atoms, the results obtained here are in much better agreement with experimental findings.

Keywords: Thin films; grand canonical Monte Carlo; molecular dynamics; surface force experiments

INTRODUCTION

Considerable advances have been made recently in the new field of nano-tribology, *i.e.* the investigation of interfacial processes on the atomic scale

*Author to whom correspondence should be addressed.

[1]. Among these, the Surface Force Apparatus (SFA) experiments of Israelachvili and co-workers [2] performed on thin films of molecular dimensions confined between two parallel surfaces has attracted much interest. SFA experiments are fascinating because they allow a direct study on a molecular scale of the-yet poorly understood-friction and lubrication phenomena.

Both static and dynamic properties of thin fluid films have been studied by SFA. The equilibrium force between the parallel surfaces as a function of separation (the so called solvation force) was shown in many cases to be a damped periodic oscillatory curve [3]. This was attributed to a smectic-like arrangement of the molecules in the ultra thin film (the tendency to form layers parallel to the surface, even though the molecules may have a quasi-spherical shape). The observed oscillation in the solvation force would thus reflect the addition or removal of whole layers of fluid. Such thin films also exhibit the so called 'stick-slip' motion when one of the walls is sheared past the other [3]. This dynamic property is often attributed to a periodic shear-melting transition and recrystallisation of the confined film during the motion [4].

Different kind of computer simulations have been performed [4–9] with the aim of reproducing the main experimental features and help in understanding the basic physics that underlines the unusual properties of thin films of molecular dimensions. Both Molecular Dynamics (MD) and Monte Carlo (MC) studies have shown the important effect of the wall structure on the properties of the confined thin films. In most of these previous studies, the simulation model consisted of a monoatomic fluid (usually Lennard-Jones (LJ) Argon) confined between rigid walls of like atoms. This type of model is of course oversimplified in many respects. For instance, oscillatory solvation force and dynamic stick-slip motion were observed experimentally with several non polar molecular fluids [3]. In the case of quasi-spherical molecules, the same solid surfaces (mica sheets) were used but the size of the molecules in the film were appreciably different (octamethylcyclotetrasiloxane (OMCTS) and cyclohexane for instance [3]). Thus a full explanation of the peculiar static and dynamic properties of confined ultra thin films should at least take into account the fact that, for these properties to be observed, the crystal structure of the solid surfaces does *not* have to be strictly compatible with the structure of the molecular film.

In this paper, we investigate by Grand Canonical Monte Carlo (GCMC) and Molecular Dynamics (MD) simulations, the equilibrium properties of a model system in which there is no strict commensurability between the structure of the wall and that of the fluid species. The dynamic properties of

this system will be described elsewhere [10]. To model such a system we simply use two different LJ atoms for the wall and the fluid atoms. We show in this paper that such a model exhibits static equilibrium properties which are closer to the SFA results for real systems than the oversimplified model in which the walls and the fluid are made of like atoms (which we will refer to, hereafter, as the 'commensurate model').

In the remainder of this paper we describe the 'incommensurate' model used in the GCMC simulations, present and discuss the results designed to mimic the static SFA experiments.

THE MODEL AND THE SIMULATION METHOD

The simulation model is depicted in Figure 1. It consisted of N fluid atoms confined between two walls, each composed of N_w atoms rigidly fixed in the configuration of the (100) plane of the face-centred-cubic (fcc) lattice. The walls were parallel to the xy plane and were a distance h apart. The walls were in complete alignment in these simulations. In most of the simulations, each planar surface consisted of 6*6 unit cells ($N_w = 72$ atoms). Several simulations were also made with 12*12 unit cells ($N_w = 288$ atoms). No significant differences were found in the results obtained between these two sets of simulations. Periodic boundary conditions were imposed in the x and y directions.

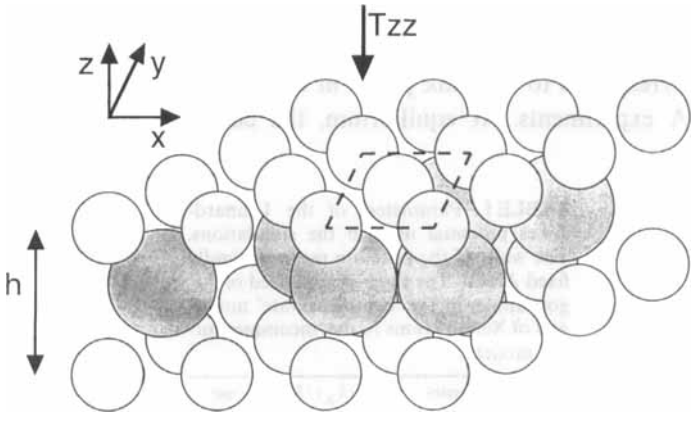

FIGURE 1 Schematic view of the model slit pore used in the simulations. The fluid atoms (shaded spheres) are confined between two parallel surfaces composed of atoms (open spheres) fixed in the configuration of the (100) plane of the fcc lattice.

The potential energy U of the system was a pairwise sum of Lennard-Jones potentials $u(r_{ij})$:

$$U = \sum_{i=1}^{N-1} \sum_{j=i+1}^{N} u_{ff}(r_{ij}) + \sum_{i=1}^{N} \sum_{j=1}^{2N_w} u_{fw}(r_{ij}) \tag{1}$$

where $u_{ff}(r_{ij})$ and $u_{fw}(r_{ij})$ are the pair potential for the fluid-fluid atoms interaction and fluid-wall atoms interaction respectively (there were no direct interaction between the walls in this model):

$$U_{fk}(r_{ij}) = 4\varepsilon_{fk}\left[\left(\frac{\sigma_{fk}}{r_{ij}}\right)^{12} - \left(\frac{\sigma_{fk}}{r_{ij}}\right)^{6}\right] \tag{2}$$

Where k stands for the fluid(f) or wall (w) species.

In our 'incommensurate' model, the fluid-fluid and fluid-wall interatomic interactions were modelled using different σ and ε values. The values are given in Table I. The wall atoms correspond to LJ-Argon and the fluid ones to LJ-Xenon. These were chosen in order to mimic the static SFA experiments of OMCTS molecules confined between mica sheets in which it is believed that the size of the quasi-spherical molecule is larger than the size of the adsorption site. Some simulations have also been performed using a 'commensurate' model, in which the walls and the fluid were composed of like LJ-Argon atoms. The parameter values for this model are also given in Table I. A cut-off radius $r_c = 3{,}5\ \sigma$ was used in all simulations. This latter model is equivalent to the one used by Diestler *et al.*, in a previous work [6].

The standard GCMC method is particularly suitable for studying the equilibrium properties of the confined fluid film. The Grand Canonical reservoir corresponds to the bulk phase in which the slit-pore is immersed in the SFA experiments. At equilibrium, the chemical potentials of the

TABLE I Parameters of the Lennard-Jones potential used in the simulations. The walls of the pore are made of rigidly fixed Argon. The fluid is composed of Argon atoms in the 'commensurate' model, and of Xenon atoms in the 'incommensurate' model

interacting pairs	$(\varepsilon/k_B)/K$	σ/nm
Argon-Argon	118.9	0.341
Argon-Xenon	159.9	0.383
Xenon-Xenon	215.0	0.425

confined and the bulk phases are equal. GCMC simulations enable to calculate the average number of molecules $\langle N \rangle$ in the slit-pore, for given values of the chemical potential, temperature and distance between planes. Three different Monte Carlo trials are attempted in a GCMC simulation: translational displacements of a randomly chosen atom within the system (canonical trials in the original Metropolis algorithm), creations of a new atom (at random position) and attempts to delete an existing atom. The acceptance criteria for all these Monte Carlo trials are such that atomic configurations are generated within the Grand Ensemble formalism with probabilities proportional to their Boltzmann weighting factor.

The solvation force is equal to $-T_{zz}$ (the component of the stress tensor). It was computed from GCMC simulations through:

$$T_{zz} = \frac{1}{A}\left\langle \sum_{i=1}^{N} \sum_{j=1}^{N_w} \left(\frac{du_{fw}(r_{ij})}{dr_{ij}} \right) \frac{z_{ij}}{r_{ij}} \right\rangle \tag{3}$$

where A is the area of each planar wall.

Structure factors $S(k_x, k_y)$ have also been computed through :

$$S(k) = \left(\frac{1}{N}\right) \left| \sum_j e^{ikr_j} \right|^2 \tag{4}$$

As shown below in the results section, several interesting equilibrium structures of the model film were observed for distinct values of h, the separation between the solid walls. In order to examine the dynamic properties of these equilibrium states of the film, we have fixed the number of film atoms N to the most probable value obtained by GCMC after equilibrium was reached, and performed standard microcanonical MD simulations for each of these states. A velocity Verlet algorithm, a time step of 5 fs, and periodic boundary conditions in the x and y directions were used in these simulations. Diffusion coefficients were computed from the slope of the mean square atomic displacement in the xy plane against time.

RESULTS AND DISCUSSION

The computed solvation force as a function of the reduced separation between the walls h^* ($h^* = h/\sigma$), at given reduced temperature and chemical potential, is shown in Figure 2 for both the 'incommensurate' and the 'commensurate' models described in the previous section. The curve obtained

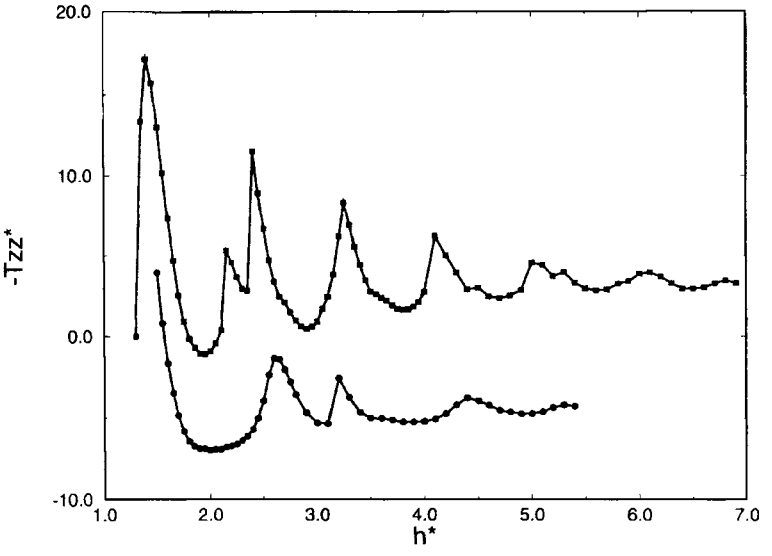

FIGURE 2 The computed reduced solvation force $-T_{zz}^* = -(T_{zz}\sigma^3/\varepsilon)$ as a function of the reduced separation between the rigid walls h^* ($h^* = h/\sigma$), at a reduced temperature $T^* = (kT/\varepsilon) = 1.00$ and a reduced chemical potential $\mu^* = (\mu/\varepsilon) = -11.00$. The top curve corresponds to the incommensurate model, the bottom one to the commensurate model. Note that, for sake of clarity, the bottom curve is shifted to lower solvation forces by a constant value of 5 T_{zz}^* units.

In this figure, $h^* = h/\sigma_{Xe-Xe}$ and $-T_{zz}^* = -(T_{zz}\sigma_{Xe-Xe}{}^3/\varepsilon_{Xe-Xe})$ for the top curve, where $h^* = h/\sigma_{Ar-Ar}$ and $-T_{zz}^* = -(T_{zz}\sigma_{Ar-Ar}{}^3/\varepsilon_{Ar-Ar})$ for the bottom curve. The solid line is a guide to the eye.

for the commensurate Ar/Ar model is in quantitative agreement with the one obtained by D. Diestler *et al.*, [6] using the same model with similar temperature and chemical potential conditions. An oscillatory solvation force is obtained in both cases. Simulations for the incommensurate model have been performed in increasing and decreasing values of h^*. No difference was found between the two sets of simulation. As already mentioned by Diestler *et al.*, [6] the oscillation in the solvation force for the commensurate model reflects the addition or removal of whole layers of fluid. In the case of the incommensurate model, an additional phenomenon is observed in the range of surface separation $2.0 \leqslant h^* \leqslant 2.5$. In this h^* range the addition of a second layer to the fluid film, in increasing the surface separation, is a two-step process. The peak at $h^* = 2.1$ corresponds to the formation of a solid bilayer body-centred-cubic film. This is followed, at $h^* = 2.4$, by a peak of larger amplitude which corresponds to a solid-solid phase transition in the bilayer film (body-centred-cubic to triclinic). We have sketched in Figure 3 the average equilibrium number of atoms in the film as a function of h^*. The addition of a

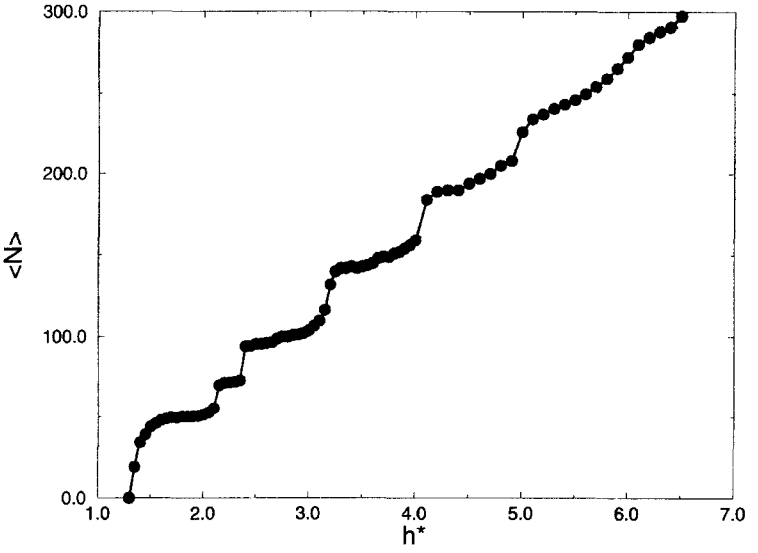

FIGURE 3 Average equilibrium number of adsorbed atoms in the film as a function of the surface separation h^*, for the incommensurate model. In this simulation, each wall consisted of 6*6 unit cells of Argon. A full layer roughly corresponds to ~50 Xenon atoms. The simulation was performed at $T^* = 1.00$ and $\mu^* = -11.00$.

second layer (~50 atoms in this simulation) is clearly a two-step process. More details on this transition will be given below. To our knowledge, no additional peak such as the one found here at $h^* = 2.1$ was ever found in the experiments. However, if such a peak existed in a real system it might have been hidden in an SFA experiment since it is located in the unstable branch of the solvation force curve (*i.e.* the region of the curve for which T_{zz} decreases with decreasing h). For more details on this technical point, the reader is forwarded to the discussion by Horn and Israelachvili (reference 11, page 1403).

We now focus on the main peaks in the solvation force curve displayed by the incommensurate model. The peaks of maximum amplitude are located at $h^* = 1.4 \pm 0.05$; 2.12 ± 0.01 ; 3.25 ± 0.05 ; 4.10 ± 0.10 ; 5.0 ± 0.1. The variation in h^* value, from one peak to the next one, is equal to 0.90 ± 0.06. Thus the oscillation in the solvation force is periodic for this model system and the periodicity correlates well with the size of the fluid atom. This is in agreement with experiments [3, 11].

The five main maxima observed in the oscillatory solvation force curve, for the incommensurate model, correspond to solid-like films (triclinic structures, see below) while the minima correspond to liquid-like structures, as evidenced by MD simulations. This means that each solid-like film displays a melting transition in increasing h^*. A further increase in the

surface separation leads to the addition of a whole layer and the simultaneous recrystallisation of the film. Melting of the monolayer film takes place progressively from $h^* \sim 1.6$ to $h^* \sim 2.0$, and no evidence of a transition can be seen in the solvation force curve. As the film thickness increases, the melting transition is evidenced by a shoulder in the peaks of the solvation force curve (melting of the bilayer film at $h^* \sim 2.7$, of the trilayer film at $h^* \sim 3.6$, see Fig. 2). Melting of the 4 and 5-layers films is evidenced by small secondary peaks at $h^* = 4.5$ and $h^* = 5.3$. For h^* values larger than 6.0, no phase transition occurs anymore and the film is liquid-like. This is in overall agreement with a recent experimental work of Klein and Kumacheva [12]. These authors have shown that a film of OMCTS molecules exhibited a liquid-like shear viscosity for large surface separations down to a value corresponding to seven molecular layers. When the separation was further decreased the film underwent an abrupt liquid to solid transition.

The decay of the solvation force has been examined. The peak to peak amplitude as a function of the surface separation is shown in Figure 4, it decays as e^{-h^*/σ^*}. This is in agreement both with experiments [11] and with a theoretical prediction based on the density functional theory formalism [13,14]. The observed reduced value of the characteristic decay length of the envelope α^* is equal to 1.56 ± 0.06 in the simulations. This value is

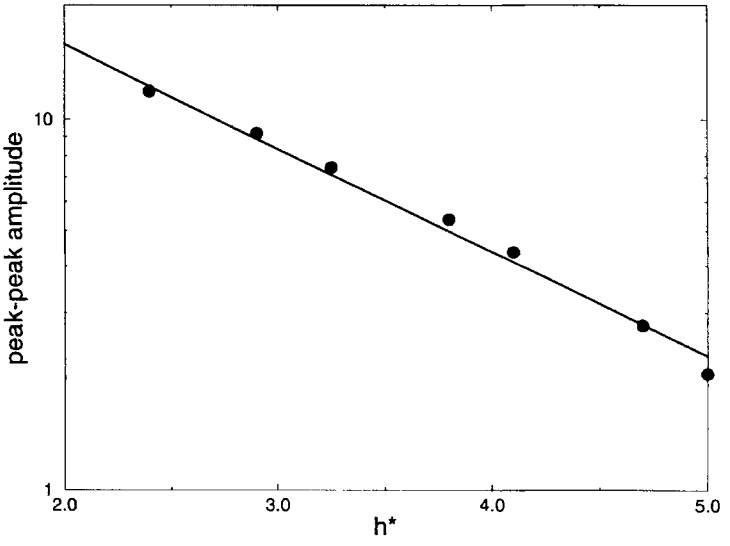

FIGURE 4 Decay of the peak to peak amplitude of the solvation force curve as a function of the surface separation h^* (semi-log scale).

somewhat larger than the oscillatory period Δh^* (0.9). Experimentally both α^* and Δh^* are close to unity [11, 15].

Despite the similarity in the shape of the solvation force curves for the incommensurate and the commensurate model (Fig. 2), the properties of these two model systems differ in many aspects. The commensurate model exhibits 5 peaks in the solvation curve, located at $h^* = 1.3$, 2.6, 3.2, 4.5 and 5.3. The variation in h^* values from one peak to next one, suggests the existence of a double periodicity in this system: $\Delta h^* \sim 1.3$ between the first and second, and third and fourth peaks, and $\Delta h^* \sim 0.7$ between second and third, and fourth and fifth peaks. This is presumably due to the fact that the films with an odd number of layers are solid-like and those with even number of layers are liquid-like, as evidenced by MD simulations (this point has been mentioned by Diestler *et al.*, [6]). The walls being in registry, no stable epitaxial solid phase having an even layer number may exist. The second and the fourth peaks are then shifted to larger values of h^*, because the density of the liquid film is lower than that of the solid. The agreement between simulations and experiments is thus poorer for the oversimplified commensurate model than for the incommensurate one.

We shall now focus on the secondary (additional) peak observed in the solvation force curve of the incommensurate model at $h^* = 2.1$. Figure 5 shows the reduced isothermal compressibility κ^*, against the surface separation h^*, where:

$$\kappa^* = \frac{\kappa \varepsilon}{\sigma^3} \tag{5}$$

κ was calculated from the density fluctuation σ_N defined as:

$$\sigma_N = \sqrt{\langle N^2 \rangle - \langle N \rangle^2} \tag{6}$$

In the Grand Canonical Ensemble, σ_N is related to the isothermal compressibility κ through:

$$\sigma_N = N\left(\frac{kT\kappa}{V}\right)^{1/2} \tag{7}$$

M. Schoen has recently shown [16] that a definition of κ in terms of density fluctuations is precluded, in general, because of the inhomogeneity of the fluid film between the structured surfaces in transverse dimensions. However, as stated by this author, such a definition is shown to be possible

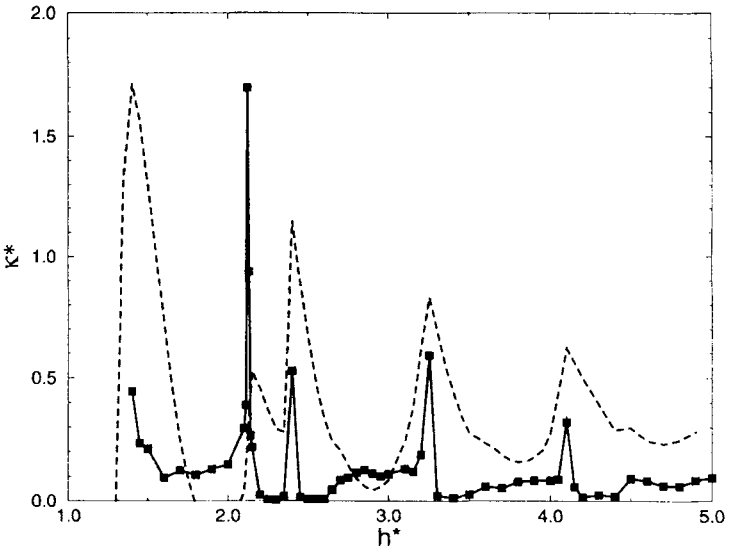

FIGURE 5 Reduced isothermal compressibility κ^* (see equations 5 to 7 in the text) against the surface separation h^* for the incommensurate model (solid line). The solvation force ($-T_{zz}^*$) is also shown (broken line). The simulation was performed at $T^* = 1.00$ and $\mu^* = -11.00$.

introducing κ as a density fluctuation-related quantity in a coarse-grained sense.

Two sharp peaks are observed in Figure 5 for h^* values of 2.1 and 2.4. They correspond to discontinuities in the second derivative of the Grand Potential. In other words, two phase transitions are observed in this h^* range. These presumably correspond to second-order phase transitions. The first peak ($h^* = 2.1$) corresponds to a liquid-solid transition and the second one ($h^* = 2.4$) to a solid-solid transition, as evidenced by the MD computation of the diffusion coefficients (Fig. 6). The mean value of the diffusion coefficient D in the separation range $1.8 < h^* < 2.1$ is $0.12\,\text{Å}^2.\text{ps}^{-1}$. This corresponds to highly confined fluid. D reaches the value of $0.17\,\text{Å}^2.\text{ps}^{-2}$ for a 10 layers confined fluid, while the computed bulk value for D is $0.23\,\text{Å}^2.\text{ps}^{-1}$. The crystallisation of the film ($h^* = 2.1$) is accompanied by a drop in the diffusion coefficient. In the separation range $2.1 < h^* < 2.6$, the bilayer film displays solid-like D values.

In the range $.26 \leqslant h^* \leqslant 3.0$, the progressive increase in isothermal compressibility (Fig. 5) and diffusion coefficient (Fig. 6), can be attributed to the melting of the bilayer film mentioned above in the discussion of the solvation force curve. As shown in Figure 5, each addition of a whole layer and simultaneous recrystallisation of the film, which takes place in increasing

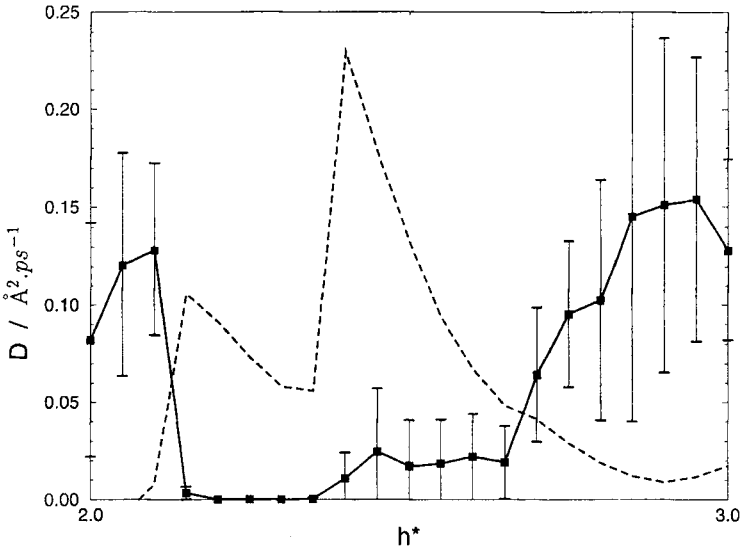

FIGURE 6 Atomic diffusion coefficients in the xy direction of the model system, computed from microcanonical MD simulations (solid line). The solvation force $(-T^*_{zz})$ is also shown (broken line). The simulations were performed at $T^* = 1.00$ and each N value was fixed as described in the text (model section).

h^* is accompanied by a well defined narrow peak in κ^*. On the other hand melting of the films appear to be much more continuous processes. No hysteresis was found when performing the simulations in increasing or decreasing the surface separation.

The structures of the two solid phases observed in the bilayer film have been investigated. The structure factor $S(k_x, k_y)$ is shown in Figure 7, together with atomic trajectories. Sharp peaks in $S(\vec{k})$, typical of crystalline phases, are obtained in both cases. In Figure 7a is shown the structure observed in the range $2.1 \leqslant h^* \leqslant 2.4$. Each layer displays a 'squared' structure and the film then corresponds to the first two (100) planes of a body centred cubic (bcc) structure. The unit cell parameters are obtained in a straighforward manner from the calculated $S(k)$. We have found $a = 0.584 \pm 0.005$ nm. In Figure 7b is shown the structure observed in the range $2.4 \leqslant h^* \leqslant 2.6$. This phase results from the packing of two hexagonal layers. Computed atomic pair distribution functions and $S(k)$ showed that the film corresponds to the first two (100) planes of a triclinic crystal. The unit cell parameters are given in Table II. In this latter phase crystallisation takes place in the $(1,-1)$ or (1,1) direction of the (100) plane of the wall. The resulting structure is more defective than the bcc one. This leads to some spread in the diffusion

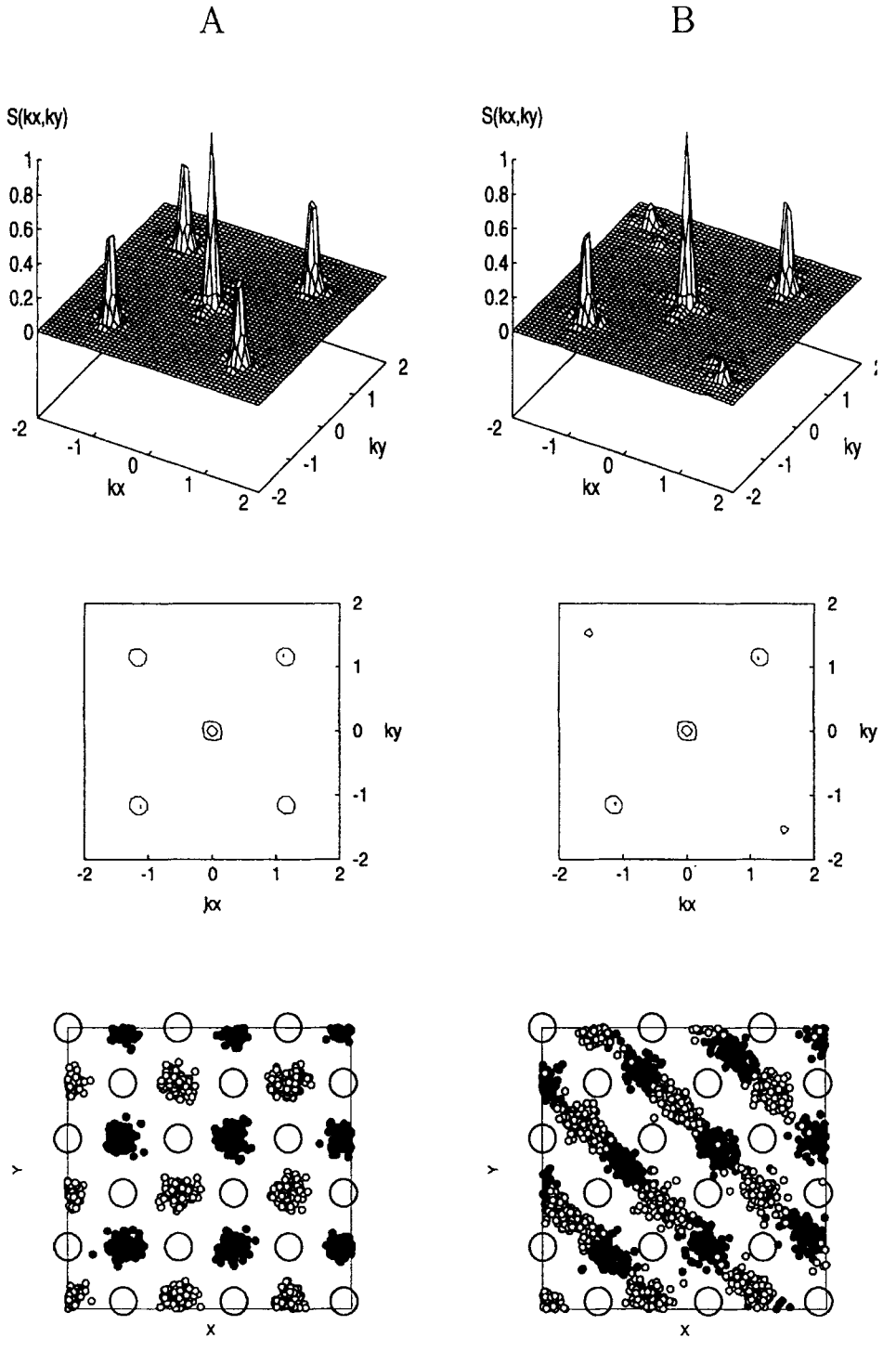

TABLE II: Unit cell parameters of the triclinic phase observed in the bilayer film, in the range $2.4 \leqslant h^* \leqslant 2.6$, with $T^* = 1.00$ and $\mu^* = -11.00$.

a/nm	0.56 ± 0.01
b/nm	0.48 ± 0.01
c/nm	0.46 ± 0.01
α/deg	52.7 ± 0.1
β/deg	52.9 ± 0.1
γ/deg	54.3 ± 0.1

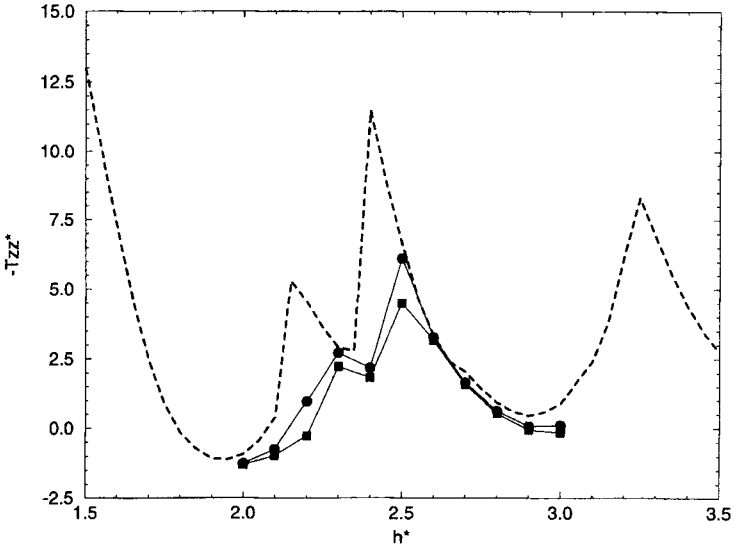

FIGURE 8 The computed reduced solvation force $-T_{zz}^*$ as a function of the reduced separation between the rigid walls h^* ($h^* = h/\sigma$), at a reduced chemical potential $\mu^* = (\mu/\varepsilon) = -11.00$ and at various reduced temperatures $T^* = (kT/\varepsilon) = 1.00$ (broken line, same as Figure 2), $T^* = 1.16$ (full circles); $T^* = 1.28$ (full squares) and $T^* = 1.40$ (full diamonds). The solid lines are guides to the eye.

FIGURE 7 Top diagrams: structure factors $S(k_x, k_y)$ for both solid phases observed in the bilayer film. Middle diagrams: projections of the structure factors in the (0, kx, ky) plane (two projections are shown for $S = 0.1$ and $S = 0.5$). Bottom diagrams: atomic MD trajectories.

A The bilayer film in the range $2.1 \leqslant h^* \leqslant 2.4$. Atomic trajectories: open circles correspond to wall atoms; full dots: atoms in the first layer; open dots: atoms in the second layer. This bilayer film corresponds to the first two (100) planes of a body centred cubic (bcc) structure.

B The bilayer film in the range $2.4 \leqslant h^* \leqslant 2.6$. Open circles (MD trajectories): wall atoms; full dots: atoms in the first layer; open dots: atoms in the second layer. This bilayer film corresponds to the first two (100) planes of a triclinic crystal. The unit cell parameters are given in Table II. All simulations were performed here at $T^* = 1.00$ and each N value was fixed as described in the text (model section).

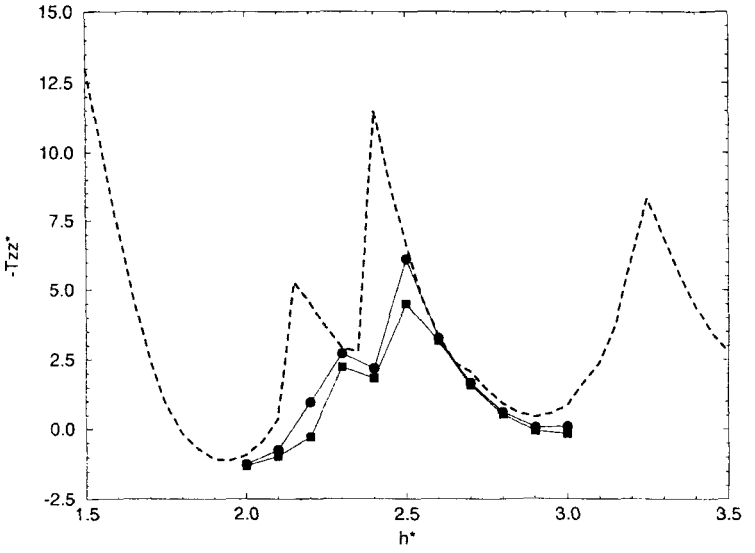

FIGURE 9 The computed solvation force $-T_{zz}^*$ as a function of the reduced separation between the rigid walls h^* ($h^* = h/\sigma$), at a reduced temperature $T^* = (kT/\varepsilon) = 1.00$ and at various reduced chemical potentials $\mu^* = (\mu/\varepsilon) = -11.00$ (broken line, same as Figure 2), $\mu^* = -12.50$ (full circles); $\mu^* = -13.20$ (full squares). The corresponding pressures of the bulk fluid are equal to P = 440, 100 and 50 bar respectively. The solid lines are guides to the eye.

coefficient in this phase, as seen above in Figure 6. Diffusion mostly takes place inside the layers. Interlayer diffusion is a rare event in the timescale of the simulation. This leads to anisotropic atomic correlations, as evidenced in the $S(k)$ data. All the other solid structures displayed by the film are triclinic (3,4 and 5−layer film at $h^* = 3.2$, 4.1 and 5.0 respectively).

Finally, the behavior of the fluid film in the range $1.5 \leqslant h^* \leqslant 3.5$ has been studied as a function of temperature and pressure (or chemical potential). The solvation force curves at various temperature (and constant pressure) and various pressure (at constant temperature) are shown in Figures 8 and 9. As the bcc-triclinic transition tends to vanish when increasing temperature or decreasing pressure, it seems that, for this model system, the bcc solid structure is a stable phase in some range of pressure and temperature only.

SUMMARY AND CONCLUSION

We have studied the behavior of confined ultra thin films of a rather simple system in which the fluid and wall particles are modelled as two different LJ rare gas atoms. This 'incommensurate' model was designed to mimic the

static SFA experiments in which it is known that epitaxy is not necessary for inducing an oscillatory solvation force in simple non polar liquids. We have indeed been able to simulate, using this simple system, many aspects of the equilibrium properties observed in the experiments. The solvation force was found to be an exponentially damped, periodic curve. All peaks of maximum amplitude in the solvation force correspond to solid-like structures. These structures progressively melt in increasing the surface separation. A further increase of h^* leads to the addition of a whole layer and the recrystallisation of the film. This latter process corresponds to a second order-like phase transition. At surface separations larger than six layers no phase transition is observed anymore and the film is liquid-like. This is also in qualitative agreement with experiments. These results suggest that the periodicity in the solvation force results from the fact that the addition of a whole layer of particles always leads to the formation of similar structures (solid-like in this case). This would enable to explain why the 'commensurate' model cannot exhibit a periodic solvation force curve. In this latter case no stable epitaxial solid phase having an even layer number may exist. Indeed, the simulations showed that films with an odd number of layers are solid-like and those with even number of layers are liquid-like in the commensurate model.

In addition the incommensurate model displayed an interesting phenomenon of confinement induced solid-solid phase transition. Two different stable packing (bcc and triclinic) have been observed in the bilayer film as a result of the competition between the fluid-wall and fluid-fluid interatomic interactions. Both structures have been observed, at some temperature and chemical potential conditions, and a transition from one to the other occurred when the surface separation was changed. At high temperature and low pressure, the phase transition vanished and the only stable packing for the bilayer film seemed to be the triclinic one. In the temperature and chemical potential range studied here, all the other solid structures (3,4 and 5-layer film) displayed by the film were also triclinic. The complete phase diagram for such an incommensurate model system is presumably rather complex. Real molecular fluid confined between mica sheets also form incommensurate systems which are expected to display several stable and/or metastable packing. However, such phase transition phenomena seem not to have been observed in the static SFA experiments. One reason for this might be that these transitions could take place in the unstable branch of the surface force curve, and the resulting additional oscillations would be hidden in the SFA experiments. It may also be that some slight change in the registry of the walls takes place during

compression in the SFA experiments. Whether or not this phenomena would drastically modify the phase diagram of the fluid system is an open question.

Our present understanding of the physics of confined ulltra thin films is obviously far from complete. However, the fact that the use of a simple incommensurate model system in the simulations enables to better reproduce some of the peculiar properties observed in SFA experiments seems encouraging. In a forthcoming paper [10] we shall describe the dynamic shearing properties of the incommensurate model described in this paper and show that it allows to simulate some important properties of the real systems. Again we show that the commensurate model fails to reproduce the basic physics of these systems. M. Schoen and co-workers [7, 17] came to a similar conclusion recently, using a different incommensurate model.

What is still open for future simulation studies is the question of how to model realistically an heterogeneous interface. Several characteristic properties of the real systems have been neglected in our model: the molecular orientational degree of freedom of the fluid species, the coulombic and induced terms in the interaction potential between the fluid and wall species, the atomic-scale flexibility of the walls, possible fluctuations in registry of the surfaces, etc...It has been shown recently that rather accurate potential functions are needed in order to reproduce all the confinement effects on the thermodynamics, structure and phase transitions of adsorbed fluids in zeolite micropores [18, 19]. Future works will tell how important this is for understanding the basic physics of ultra thin confined films.

Acknowledgements

We gratefully acknowledge M. Schoen and R. Evans for fruitful discussions.

References

[1] Bhushan, B., Israelachvili, J. N. and Landman, U. (1995) "Nanotribology : friction, wear and lubrication at the atomic scale", *Nature*, **374**, 607.
[2] Yoshizawa, H., McGuiggan, P. and Israelachvili, J. (1993) "Identification of a second dynamic state durring stick-slip motion", *Science*, **259**, 1305, and references therein.
[3] Gee, M. L., McGuiggan, P. M., Israelachvili, J. N. and Homola, A. M. (1990) "Liquid to solidlike transitions of molecularly thin films under shear", *J. Chem. Phys.*, **93**, 1895.
[4] Thompson, P. A. and Robbins, M. O. (1990) "Origin of stick-slip motion in boundary lubrication", *Science*, **250**, 792.
[5] Lupowsky, M. and van Swol, F. (1991) "Ultrathin films under shear", *J. Chem. Phys.*, **95**, 1995.
[6] Diestler, D. J., Schoen, M. and Cushman, J. H. (1993) "On the thermodynamic stability of confined thin films under shear", *Science*, **262**, 545.
[7] Schoen, M., Hess, S. and Diestler, D. J. (1995) "Rheological properties of confined thin films", *Phys. Rev.* **E52**. 2587; Schoen. M., Diestler, D. J. and Cushman, J. H. (1994)

J. Chem. Phys., "Stratification-induced order-disorder phase transition in molecularly thin confined films", **101**, 6865 and references therein.
[8] Somers, S. A., McCormick, A. V. and Davis, H. T. (1993) "Superselectivity and solvation forces of a two-component fluid adsorbed in slit micropore", *J. Chem. Phys.*, **99**, 9890.
[9] Frinck, L. J. D. and van Swol, F. (1994) "Solvation force and colloidal stability: a combined Monte Carlo and density functional theory approach", *J. Chem. Phys.*, **100**, 9106.
[10] Ph. Bordarier, Rousseau, B. and Fuchs, A. H. to be published
[11] Horn, R. G. and Isrealachvili, J. N. (1981) "Direct measurement of structural forces between two surfaces in a nonpolar liquid", *J. Chem. Phys.*, **75**, 1400.
[12] Klein, J. and Kumacheva, E. (1995) *Science*, **269**, 816.
[13] Evans, R., Henderson, J. R., Hoyle, D. C., Parry, A. O. and Sabeur, Z. A. (1993) "Asymptotic decay of liquid structure-Oscillatory liquid-vapor density profiles and the Fisher-Widom line", *Mol.Phys.*, **80**, 755.
[14] Evans, R., Leote de Carvalho, R. J. F., Henderson, R. J. F. and Hoyle, D. C. (1994) "Asymptotic decay of correlations in liquid and their mixtures", *J Chem. Phys.*, **100**, 591.
[15] Isrealachvili, J. (1992) *Intermolecular and surface forces*, Academic Press, p.266.
[16] Schoen, M. (1996) "On the uniqueness of stratification-induced second-order phase transitions in confined films", Proc. of the Minisymposium on Thermodynamics of Surfaces and Interfaces, ED. by W. Muschik, C. Papenfuss (T. U. Berlin, Berlin).
[17] Schoen, M. (1996) "Computer simulation of the rheological properties of confined films", *Mol. Simulation*, in press.
[18] Pellenq, R. J-M. and Nicholson, D. (1995) "Intermolecular potential function for the physical adsorption of rare gases in silicalite zeolite", *J. Phys. Chem.*, **98**, 13339 (1994); "Grand ensemble simulation of simple molecules adsorbed in silicalite1 zeolite", Langmuir, **11**, 1626.
[19] Lachet, V., Boutin, V., Pellenq, R. J. -M., Nicholson, D. and Fuchs, A. H. (1996) "A Molecular simulation study of the structural rearrangement of methane adsorbed in aluminophosphate A1PO4-5", *J. Phys. Chem.*, in press.